JPL D-78962

Multiangle SpectroPolarimetric Imager

User Guide for the AirMSPI Level 1B2 Products

Michael J. Garay

Jet Propulsion Laboratory
California Institute of Technology

December 5, 2013

Jet Propulsion Laboratory, California Institute of Technology

Distributed by the Atmospheric Science Data Center
http://eosweb.larc.nasa.gov

Distributed by the Atmospheric Science Data Center
http://eosweb.larc.nasa.gov

JPL D-78962

Airborne Multiangle SpectroPolarimetric Imager (AirMSPI)

User Guide for the AirMSPI Level 1B2 Products

APPROVALS:

David J. Diner
AirMSPI Principal Investigator

Earl G. Hansen
AirMSPI Project Manager

Approval signatures are on file with the AirMSPI Project.
To determine the latest released version of this document, consult the AirMSPI web site (http://airbornescience.jpl.nasa.gov/instruments/airmspi/).

Jet Propulsion Laboratory
California Institute of Technology

Distributed by the Atmospheric Science Data Center
http://eosweb.larc.nasa.gov

Copyright 2013 California Institute of Technology. Government sponsorship acknowledged.

The research described in this publication was carried out at the Jet Propulsion Laboratory, California Institute of Technology, under a contract with the National Aeronautics and Space Administration.

Distributed by the Atmospheric Science Data Center
http://eosweb.larc.nasa.gov

Document Change Log

Revision	Date	Affected Portions and Description
	22 April 2013	Original release
1	5 December 2013	Updated to include description of KML files for use with Google Earth as well as changes relative to V003 of the product

Which Product Versions Does this Document Cover?

Product Filename Prefix	**Version Number in Filename**	**Brief Description**
AirMSPI_ER2_GRP_ELLIPSOID	V003	L1B2 Ellipsoid-Projected Georectified Radiance and Polarimetry Data
AirMSPI_ER2_GRP_TERRAIN	V003	L1B2 Terrain-Projected Georectified Radiance and Polarimetry Data

Distributed by the Atmospheric Science Data Center
http://eosweb.larc.nasa.gov

TABLE OF CONTENTS

1 INTRODUCTION 7

1.1 THE AIRMSPI INSTRUMENT 7
1.2 AIRMSPI DATA PRODUCTS 7
1.3 CONTROLLING DOCUMENTS 7
1.4 RELATED DOCUMENTS 7

2 AIRMSPI INSTRUMENT DESCRIPTION 8

2.1 OPTICS 8
2.2 RETARDANCE MODULATOR 8
2.3 FOCAL PLANE SPECTROPOLARIMETRIC FILTERS 9
2.4 FOCAL PLANE DETECTORS 10
2.5 ELECTRONICS 10
2.6 INSTRUMENT HOUSING 10
2.7 GIMBAL DRIVE 11
2.8 ON-BOARD POLARIZATION MONITORING AND CONTROL SYSTEMS 13
2.9 DATA ACQUISITION AND GROUND PROCESSING 14

3 WORKING WITH AIRMSPI DATA 15

3.1 DATA PRODUCT SPECIFICATIONS 15
3.2 STEP-AND-STARE PRODUCTS 15
3.2.1 File Formats 15
3.2.2 Browse Product 16
3.2.3 KML Product 17
3.2.4 Single View Angle 18
3.2.5 Content 18
3.2.6 Radiometric Data Quality Indicator (RDQI) 21
3.2.7 Polarized Intensity and Unit Conversions 22
3.2.8 Color Images 24
3.2.9 Navigation 24
3.2.10 Multiple View Angles 24
3.2.11 Matching and Overlap 24
3.2.12 Multiangle Spectropolarimetry 24
3.3 SWEEP PRODUCTS 24

4 APPENDIX 26

4.1 REFERENCES 26
ACRONYM LIST 28

Distributed by the Atmospheric Science Data Center
http://eosweb.larc.nasa.gov

1 INTRODUCTION

1.1 The AirMSPI INSTRUMENT

The Airborne Multiangle SpectroPolarimetric Imager (AirMSPI) is an 8-band (355, 380, 445, 470, 555, 660, 865, 935 nm) pushbroom camera, measuring polarization in the 470, 660, and 865 nm bands, mounted on a gimbal to acquire multiangular observations over a ±67° along-track range. The instrument has been flying aboard the NASA ER-2 high altitude aircraft since October 2010. AirMSPI employs a photoelastic modulator-based polarimetric imaging technique to enable accurate measurements of the degree and angle of linear polarization in addition to spectral intensity.

The purpose of this document is to provide guidelines for the usage of the AirMSPI L1B2 products.

1.2 AirMSPI DATA PRODUCTS

The MISR Science Computing Facility (SCF) at the Jet Propulsion Laboratory (JPL) supports the development of AirMSPI science algorithms and software, instrument calibration and performance assessment, as well as providing quality assessment and data validation services with respect to AirMSPI Science Data Processing (SDP). The MISR SCF is used to perform the standard processing of the AirMSPI data. After AirMSPI data processing is complete, the standard output products are archived and made available to users via the Langley Research Center (LaRC) Atomospheric Science Data Center (ASDC) client services.
https://eosweb.larc.nasa.gov/project/airmspi/airmspi_table

1.3 CONTROLLING DOCUMENTS

1) Multiangle Spectropolarimetric Imager (MSPI) Algorithm Theoretical Basis Document Rev. B Draft, November 2009 (or latest version).

1.4 RELATED DOCUMENTS

2) Data Product Specification for the AirMSPI Level 1B2 Products, JPL D-78958, December 2013 (or latest version).
3) AirMSPI Data Quality Statement. December 2013 (or latest version).

Distributed by the Atmospheric Science Data Center
http://eosweb.larc.nasa.gov

2 AirMSPI INSTRUMENT DESCRIPTION

2.1 OPTICS

AirMSPI is an eight-band pushbroom camera, mounted on a gimbal to acquire multiangular observations over a ±67° along-track range. The AirMSPI spectral bands are centered at 355, 380, 445, 470P, 555, 660P, 865P, and 935 nm. Those bands marked with the letter "P" provide polarimetric information. The 935-nm channel is an experimental band included to explore the possibility of retrieving column water vapor abundance using multiangle observations. AirMSPI's telescope has an effective focal length of 29 mm and cross-track field of view of ±15º. Incoming light is brought to a focus using a three-mirror f/5.6 anastigmatic, telecentric system of the same design as used in LabMSPI/GroundMSPI (Diner et al., 2010). To increase optical throughput, particularly in the UV, AirMSPI employs redesigned mirror coatings. In addition to high reflectance, design goals for the coatings included low diattenuation and low retardance (relative difference in reflectance and phase, respectively, for light polarized in perpendicular planes). Precision Asphere, Inc. fabricated the mirrors and Surface Optics Corporation applied the optical coatings. Over the entire UV-SWIR spectral range, the measured diattenuation is <0.5%, reflectance is >85%, and retardance is <10°. Because diattenuation is intrinsically low for the new coating design, the diattenuation balancing approach used in GroundMSPI (Mahler et al., 2008) was not required and each mirror was identically coated.

2.2 RETARDANCE MODULATOR

AirMSPI uses a time-varying retardance in the optical path to modulate the orientation of the linearly polarized component of the incoming light, described by the Stokes components Q (excess of horizontally over vertically polarized light) and U (excess of 45º over 135º polarized light) (Diner et al., 2007, 2010; Mahler et al., 2011a). This oscillating retardance is achieved by placing a pair of Hinds Instruments Series II/FS42 PEMs in the optical train. PEMs are fused silica plates coupled to quartz piezoelectric transducers that induce a rapidly oscillating retardance via the photoelastic effect. The fast axes of the two PEMs are aligned and nominally parallel to the long dimension of the focal plane line arrays. The AirMSPI PEMs have resonant frequencies of f_1 = 42060 and f_2 = 42037 Hz at 18ºC. These frequencies shift by about 2.6 Hz per 1ºC change in temperature, but the difference frequency $\Delta f = f_1 - f_2$ (23 Hz) is much less temperature sensitive, changing by only 15 mHz ºC^{-1}. The difference in resonant frequency of the two PEMs generates a beat signal whose period defines the duration of an image frame ($t_{frame} = 1/\Delta f$ = 43.5 ms). This beat modulation is typically sampled 23 times per frame, and the time-varying signal is processed using the algorithm described in Diner et al. (2010) to retrieve I and Q simultaneously from those pixels overlain by a polarization analyzer oriented at 0º, and I and U from those pixels overlain by a polarization analyzer oriented at 45º, where I is the first Stokes component (intensity). By virtue of this approach, the ratios $q = Q/I$ and $u = U/I$ are, to first order, insensitive to the absolute radiometric calibration of a given pixel because both the numerator and denominator are determined from signals acquired by the same detector element. The degree of linear polarization (DOLP) and angle of linear polarization (AOLP) derived from these

Distributed by the Atmospheric Science Data Center
http://eosweb.larc.nasa.gov

ratios, equal to $\sqrt{q^2+u^2}$ and $0.5\tan^{-1}(u/q)$, respectively, are similarly insensitive to absolute calibration. To compensate for instrumental polarization aberrations (e.g., mirror diattenuation, imperfect retardance), a set of 10 polarimetric calibration coefficients is established for every pixel (Diner et al., 2010). These features enable the MSPI class of instruments to meet the ACE DOLP uncertainty requirement of ±0.005 (ACE Science Working Group, 2010). Results from LabMSPI (Diner et al., 2010) and GroundMSPI (Diner et al., 2012) show DOLP uncertainties, determined as the root-mean-square residual in DOLP as a polarizer is rotated in front of the camera, of ±0.003 or better. Preliminary results for AirMSPI show similar residuals.

Quarter-wave plates (QWPs) located in the optical path before and after the PEMs results in modulation of the two desired linear Stokes vector components, *Q* and *U*. Without the QWPs, the camera would be sensitive to *U* and *V*, the latter being the excess of right-handed over left-handed circular polarization. Since *V* is typically small for natural scenes (Plass et al., 1976; Kawata, 1978), measurement of this Stokes component is sacrificed in order to obtain sensitivity to both *Q* and *U*. In the single-band LabMSPI camera, zero-order quartz QWPs were used. For GroundMSPI, these were replaced with commercial QWPs constructed from quartz and magnesium fluoride (MgF_2). Custom QWPs were designed and fabricated to meet the more stringent AirMSPI performance requirements (Mahler et al., 2011b). The design goal was to achieve retardance within ±10° of 90° (one quarter wave) in the polarimetric bands and <0.1° retardance change with 1°C change in temperature. The use of a composite, three-element retarder provides three degrees of freedom, two of which were designated for the shape of the retardance curve and the third for athermalization. The three materials employed are quartz, MgF_2, and sapphire. Karl Lambrecht Corporation assembled the AirMSPI compound retarders. Nominal retardance is 90º, 92º, and 86º, respectively, at 470, 660, and 865 nm. Deviations of QWP performance from exact quarter-wave and the effect of finite spectral bandwidth are accounted for in the coefficients derived as part of the polarimetric calibration process (Diner et al., 2010).

2.3 FOCAL PLANE SPECTROPOLARIMETRIC FILTERS

Nominal full width at half maximum (FWHM) bandpasses of AirMSPI's eight spectral bands in order from UV to NIR are 29, 33, 38, 39, 29, 39, 38, and 50 nm, respectively. Intensity measurements in the near-UV are beneficial because most surfaces are dark at these wavelengths, and the interaction between aerosols and enhanced Rayleigh scattering provides sensitivity to aerosol height (e.g., Torres et al., 2002). Sensitivity studies suggest that polarization channels in the UV would not offer significant benefits for aerosol retrievals due to the dominance of polarization by the molecular atmosphere (Kalashnikova et al., 2011), so only intensity data are acquired in this spectral region. Visible and near-infrared intensity and polarization measurements provide sensitivity to particle size and complex refractive index. The longest-wavelength channel of AirMSPI is located in a water vapor absorption band.

To provide spectral and polarimetric selection for different rows of the photodetector line arrays, the AirMSPI spectral filters were sliced into thin strips (80 μm wide by 17 mm long), bonded together, and polished. Materion Barr Precision Optics designed and fabricated this "butcher block" filter. High optical density black epoxy is used between the spectral filters for stray light reduction. The assembly was bonded to a fused silica substrate containing patterned wire-grid polarizers (WGPs) in the

Distributed by the Atmospheric Science Data Center
http://eosweb.larc.nasa.gov

polarization channels. Moxtek, Inc. supplied the WGPs. Application of a cement bond to the WGPs results in reduced transmittance and polarization extinction ratio (ratio of transmittance of the polarization state aligned with polarizer to the transmittance for the orthogonal state) relative to their pre-bond values. The use of high-contrast WGP stock results in post-bond transmittance exceeding 75% and extinction ratios between 40 and 100, depending on wavelength. The extinction ratio determines the magnitude of the modulation pattern from the PEMs, and is readily accounted for in instrument calibration. A Mueller Matrix Imaging Polarimeter (MMIP) at the University of Arizona was used for inspection and characterization of the spectropolarimetric filter components. Alignment and bonding of the filter to the silicon complementary metal oxide semiconductor (Si-CMOS) imager was done at the Jet Propulsion Laboratory (JPL). The composite filter assembly is situated above the detector array in the camera focal plane. The precision positioning equipment used to accomplish this step is able to ensure alignment to within ±2 μm over the 17-mm length of the filter.

2.4 FOCAL PLANE DETECTORS

Both the GroundMSPI and AirMSPI instruments use the same Si-CMOS line array detectors. JPL designed the detectors and readout integrated circuits. These devices are sensitive to light in the UV/VNIR spectral range. Sixty-four lines on 16 μm spacing contain 1536 pixels with 9.5 μm (cross-track) x 10 μm (along-track) apertures. Tower Semiconductor, Ltd fabricated the detector array. Top-level characteristics are shown in Table 1. Reset noise is minimized through the use of correlated double sampling (CDS), in which the values on all capacitors are digitized and read out at the start of each integration interval and temporarily stored off chip and then subtracted from the integrated values as they are read out. All 1536 pixels in a given row are integrated in parallel.

2.5 ELECTRONICS

AirMSPI electronic circuits were designed and built to meet dual-PEM polarimeter signal timing and phasing requirements outlined in Diner et al. (2007). Polarimetric accuracy is maximized by properly sampling the video signal and by synchronizing the sampling with the retardance modulation of the dual PEM. Each of the two AirMSPI PEM controllers drives an all-digital phase locked loop (PLL). This enables the phase of each PEM to be available at all times. Synchronization to the high frequency modulation and low beat frequency is accomplished by computing the sum and difference of the two PEM phases. In GroundMSPI, the support electronics are divided between a Focal Plane Array (FPA) board and a Data Recovery Board (DRB) (Diner et al., 2012). For AirMSPI, these circuits were combined into a single focal plane control and processing (FPCP) board that makes use of a Xilinx military-grade Virtex-5FXT field programmable gate array (FPGA) in place of the Spartan-3 used in GroundMSPI. Wide dynamic range is made possible by the large detector full well and 9-bit nonlinear quantization during each image frame. When all samples are combined over a frame the effective quantization is nearly 16 bits.

2.6 INSTRUMENT HOUSING

The AirMSPI housing reuses much of the hardware developed for its non-polarimetric precursor, AirMISR (Diner et al., 1998b). The camera is mounted on a gimbal to permit multi-angle imaging. Like AirMISR, the housing containing the AirMSPI gimbal assembly is mounted in the nose of the

Distributed by the Atmospheric Science Data Center
http://eosweb.larc.nasa.gov

NASA high-altitude ER-2 aircraft. As shown in Fig. 1, the aluminum cylinder assembly protrudes below the aircraft fuselage. A pressure box around the gimbal assembly maintains 276 hPa (4 psi) pressure inside the nose compartment, and the sensor head experiences outside ambient pressure (~48 hPa or 0.7 psi at 20 km altitude). The camera and rotary stage cabling is led out through a set of pressure bulkhead connectors to the instrument electronics rack. The ER-2 supplies 28 VDC power to the instrument. The instrument draws ~181 W of power during data acquisition, with an additional 70 W worth of independent heaters distributed through the camera volume to ensure that the instrument temperature does not drop below the dew point during aircraft descent. Re-engineering of the electronics and data system layout reduced instrument mass from ~170 kg for AirMISR to 86 kg for AirMSPI.

Figure 1. Left: Pressure vessel and cylindrical drum housing the AirMSPI camera. Right: AirMSPI in its current installation in the nose of the ER-2. The instrument is visible protruding below the fuselage.

2.7 GIMBAL DRIVE

In transitioning from AirMISR to AirMSPI, the gimbal and motor drive were upgraded to a system (Aerotech WaferMax T-RE2048AS) having much higher torque and a precision angle encoder, enabling more flexible operating and camera pointing modes (AirMISR acquired imagery at only a predefined set of nine view angles). The gimbal enables image acquisition at a programmable set of along-track angles between ±67º. While it is possible to acquire observations at larger view angles, aircraft attitude fluctuations significantly degrade the quality of the imagery. Sequences to be used during a given flight are pre-programmed on the ground, and are constructed from two basic operating modes, illustrated in Fig. 2. In "step and stare" mode, the camera is pointed at the same target area at a fixed set of view angles beginning with the most forward view and then stepping aftward as the aircraft flies downtrack. The camera then slews forward and the sequence repeats for the next target, about 100 km downtrack. This mode is most useful where the highest possible spatial resolution (~10 m) is desired. Target area is ~10.6 km cross-track (at nadir) x 9.5 km along-track for a nominal sequence containing nine view angles. An odd number of "stares" is typically selected so that the images are acquired for a set of symmetric view angles forward and aftward of the nadir (0°) view angle. The along-track sample spacing (8 m at any angle) is set by the frame time and aircraft speed. In "continuous sweep" mode, the gimbal slews back and forth. Because the gimbal moves

Distributed by the Atmospheric Science Data Center
http://eosweb.larc.nasa.gov

continuously, spatial resolution is reduced to ~55 m due to smear. However, this mode enables better spatial coverage of multi-layered cloud fields. AirMSPI's actuator permits the slew rate to vary as a continuous function of angle in order to keep the amount of image smear constant at all angles.
A variant of the first operating mode, dubbed "step and pseudostare," is made possible by the programmable nature of the AirMSPI actuator. During each of the "stare" portions of the sequence, the gimbal drifts forward at a slow rate (between a few hundredths and a few tenths of a degree per second, depending on view angle), enabling extension of the along-track length of the observed target areas. For example, without the drift, overlap imagery of nine multi-angle views can be obtained with a 9.5 km target length, as noted above. Allowing a small amount of forward drift in the view angle during image acquisition introduces only 2 m of along-track smear and extends the target length to 11.5 km. This mode has been successfully tested in flight. Acquisition of step and pseudostare imagery at up to 31 view angles has been demonstrated.

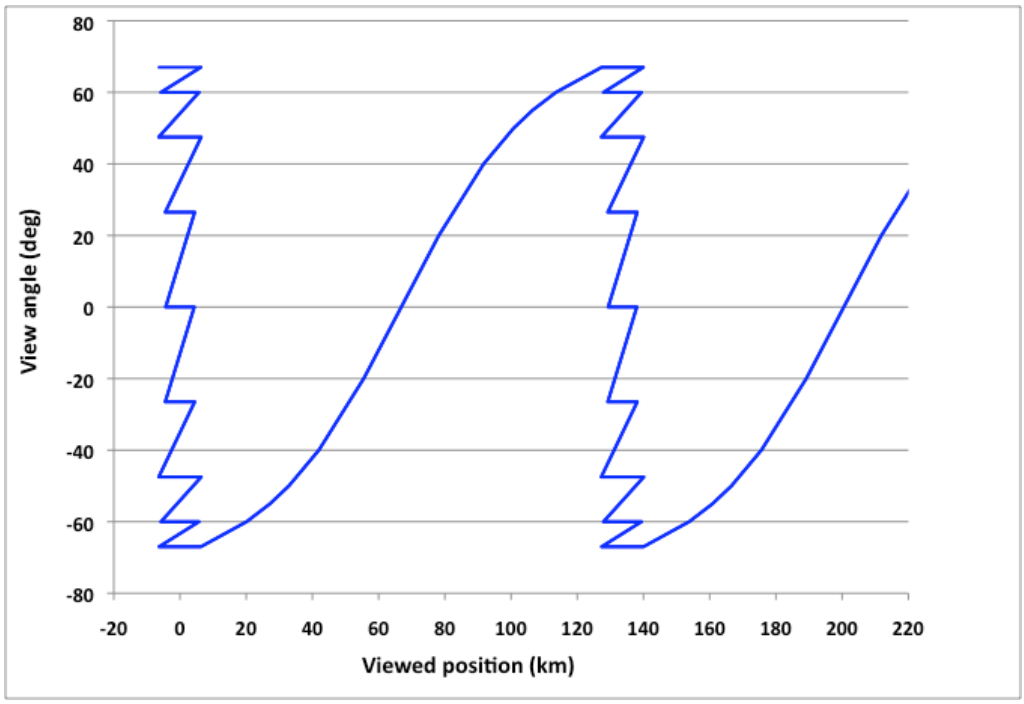

Distributed by the Atmospheric Science Data Center
http://eosweb.larc.nasa.gov

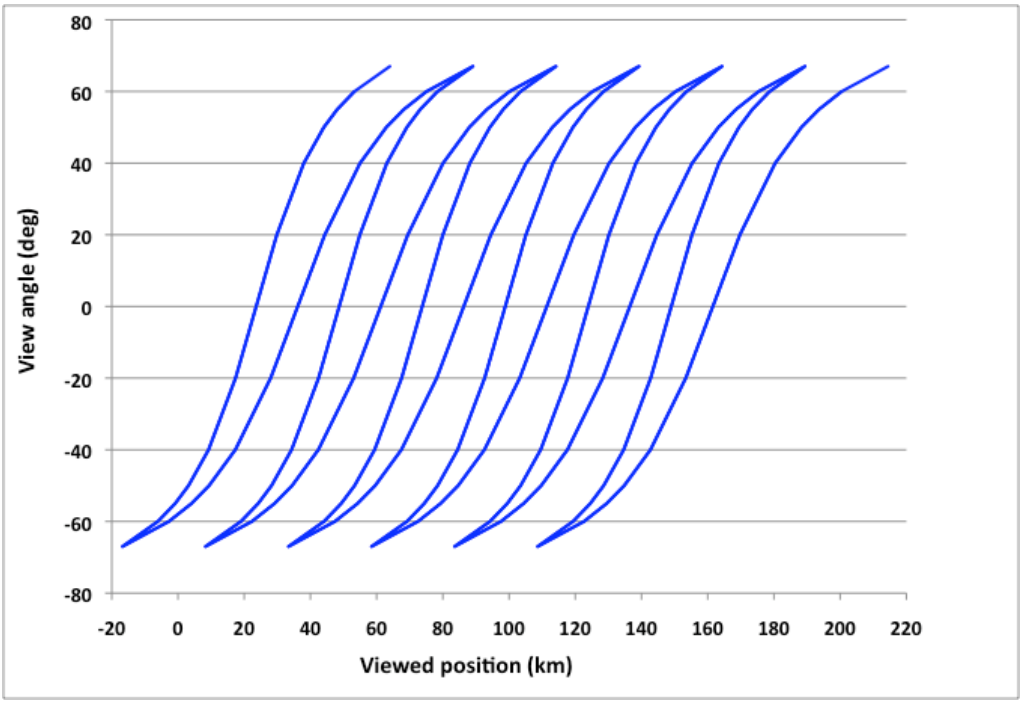

Figure 2. Top: Example of the AirMSPI "step and stare" mode, with nine view angles, showing view zenith angle at the center of the camera field of view as a function of viewed downtrack position on the ground. Bottom: In "continuous sweep" mode, the gimbal slews back and forth providing variable view angles and wider areal coverage than possible in step and stare mode.

2.8 ON-BOARD POLARIZATION MONITORING AND CONTROL SYSTEMS

Two specialized pieces of equipment for verifying and controlling the performance of the polarimetric measurement approach during in-flight operations of AirMSPI were developed and implemented. The first is a simple polarization "validator." Although the temperature sensitivity of QWP retardance has been minimized by design, as described above, it is still possible that the retardance may shift somewhat due to temperature changes during flight. Illumination of the camera with light polarized at 0º, 15º, 60º, and 75º provides a useful means for determining the deviations of the polarization calibration coefficients from their nominal values as a result of QWP retardance shifts. A source of light linearly polarized in these different orientations was designed and constructed for the AirMSPI camera to view in flight. This source consists of nine light-emitting diodes (LEDs), three each at the AirMSPI polarimetric wavelengths. These illuminate a plastic diffuser. In front of this source, sheet polarizers at the required orientations were installed, and this assembly was integrated into the AirMSPI instrument. The validator is viewed by rotating the gimbal forward to an angle of 87º. The LEDs flash for 1 second every 10 seconds so that dark data can be collected between the illumination flashes. Validator data have been used to evaluate the in-flight PEM retardance and phase control system, known as the "optical probe."

The optical probe sends a beam of light through the PEMs to monitor their retardances and phases. The beam traverses the PEMs in an area not used for acquisition of Earth imagery. The light source in

Distributed by the Atmospheric Science Data Center
http://eosweb.larc.nasa.gov

the optical probe is a 760 nm LED, and a combination of two linear polarizers and a QWP generates the required optical signals. The digitized output is synchronously demodulated and the system generates error signals showing how far the PEM retardances and phases are from their desired values. Four quantities are determined: the mean retardance of the two PEMs, the difference in retardance between the two PEMs, the phase of the low-frequency beat pattern, and the phase of the high-frequency oscillation. The feedback control system then adjusts the PEM parameters to drive the error signals to zero. The same Virtex-5FXT FPGA that operates the rest of the AirMSPI camera performs probe data acquisition and processing. During an AirMSPI flight on 31 August 2011, the probe was operated open loop (i.e., the PEMs were monitored but not controlled). Subsequently, a feedback algorithm was implemented to enable closed-loop operation, which was first used during a flight on 6 January 2012. Analysis of imagery of the light flashes from the onboard validator hardware enabled an independent measure of PEM retardance. The resulting data demonstrated the ability to control the PEM retardance and phase parameters to within a fraction of 1 mrad, keeping contributions to the overall DOLP uncertainty budget at <0.001.

2.9 DATA ACQUISITION AND GROUND PROCESSING

Flight control software consists of data acquisition routines, gimbal operation instructions, and a main program. A Condor CEI-200 two-channel ARINC-429 board in the AirMSPI on-board computer receives ER-2 attitude and position data. The original AirMISR on-board data system was upgraded by replacing the hard disks with solid state memory and adding a CameraLink data collection system. An IO Industries frame grabber and disk shuttle packs are used. The current 4x256GB Serial Advanced Technology Attachment (SATA) solid-state drives (SSDs) provide ~1TB of memory, enabling storage of ~10 hours of data. The SSDs are exchangeable after a flight within minutes, allowing the instrument to be immediately flight-ready for a follow-up mission.

Accurate position and attitude data are required for georectification and co-registration of the different channels of AirMSPI data. The camera acquires image data in pushbroom fashion (one image line at a time for each channel). Image lines (frames) are acquired at a rate of 23 Hz. To georectify and co-register the acquired imagery with subpixel accuracy, aircraft position and attitude data are used to define the viewing geometry of each image line. A two-channel ARINC-429 board in the AirMSPI onboard computer receives attitude and position data at 64 Hz from the ER-2's inertial navigation/global positioning system (INS/GPS) to meet ground data processing requirements for image navigation (Jovanovic et al., 2001, 2012).

Data product generation makes use of the AirMSPI Data Processing System (AMDPS), which employs software developed for AirMISR (Jovanovic et al., 2001) and MISR (Jovanovic et al., 2002). Level 1A1 processing reformats the raw AirMSPI output into Hierarchical Data Format (HDF). Level 1A2 performs data conditioning, such as compensation for detector nonlinearity and dark level subtraction. Level 1B1 extracts the Stokes parameters *I, Q,* and *U* and their linear gradients during each image frame, and applies pixel-by-pixel radiometric gain coefficients. Level 1B2 spatially co-registers the channels, maps the observations to the surface terrain, corrects for residual instrument polarization, and derives DOLP and AOLP relative to both the view meridian plane (the plane containing the view vector and the surface normal) and the scattering plane (the plane containing the view vector and the solar illumination vector).

Distributed by the Atmospheric Science Data Center
http://eosweb.larc.nasa.gov

3 WORKING WITH AirMSPI DATA

3.1 DATA PRODUCT SPECIFICATIONS

AirMSPI Level 1B2 Products contain radiometric and polarimetric observations of clouds, aerosols, and the surface of the Earth made from the National Aeronautics and Space Administration's (NASA) ER-2 high altitude research aircraft. The AirMSPI instrument acquires data using one of two possible modes, step-and-stare and sweep. Step-and-stare data are gridded at 10 m spatial sampling, with one file provided for each view angle. Sweep data are gridded at 25 m spatial sampling. Files are distributed in HDF-EOS-5 format. Details of the contents of these files can be found in the Data Product Specification for the AirMSPI Level 1B2 Products document.

3.2 STEP-AND-STARE PRODUCTS

As described above, the AirMSPI gimbal allows operation of the instrument in two primary modes. In the step-and-stare mode the gimbal is moved to a specific angle causing the camera to point in a particular direction (stare) and the motion of the aircraft causes the line arrays to sweep out an image. The gimbal then moves to another position (step), aftward of the first to allow coverage of a similar location on the ground as the aircraft moves forward, and the stare is repeated. Note that operationally the "step-and-pseudostare" is more typically used, which uses a slow gimbal motion during the "stare" to extend the along-track length of the target area. More information on this mode and the gimbal can be found in Section §2.7.

This section provides details related to working with products produced using the step-and-stare mode.

3.2.1 File Formats

The L1B2 step-and-stare products are distributed in HDF-EOS-5 format. Associated browse images are provided to users in JPEG format as well as KML files for use with Google Earth; both these types of products are described in more detail below. A single "target" observed in step-and-stare mode will typically have nine files associated with it, accounting for each of the individual stares. However, the number of stares in a target sequence may vary from as few as five to as many as 31. Typically an odd number of stares are specified to include a nadir (0° downward) view and a symmetrical number of views in both the forward and aftward directions.

Files belonging to a single target can be identified by the target name included in the filename (e.g., "Hanford") and a sequence of associated times and angles. The times included in the filename represent the UTC time (YYYMMMDD_HHMMSSZ) of the midpoint of the image acquisition, progressing from the most oblique forward view to the most oblique aftward view. The mean view angle of the acquisition is also included in the filename in decimal degrees multiplied by ten followed by a letter designating the viewing direction relative to aircraft motion F=forward, N=nadir, A=aft. Thus, a designation of 660F represents a mean view angle of 66.0° with the camera oriented in the forward direction relative to the motion of the aircraft. The time difference between views varies from angle to angle, but is generally less than 60 s for the standard nine-view sequence. The time

Distributed by the Atmospheric Science Data Center
http://eosweb.larc.nasa.gov

difference between subsequent step-and-stare targets, identified by different target names, is typically longer than 60 s.

3.2.2 Browse Product

Figure 3 shows the browse image created for the 0° (nadir) step-and-stare acquisition over Hanford, CA on 18 January 2013 during the PODEX field campaign. The six panels provide users a quick view of the image contents and the different spectral and polarimetric information provided by AirMSPI. Note that these images are cropped to maximize the amount of image data, and an automatic histogram stretch is applied to enhance the appearance of the imagery, which makes quantitative assessment of the image content difficult using the browse images alone. However, the browse images are provided at the full spatial resolution of the data (10 m for the step-and-stare mode), so fine spatial details are retained.

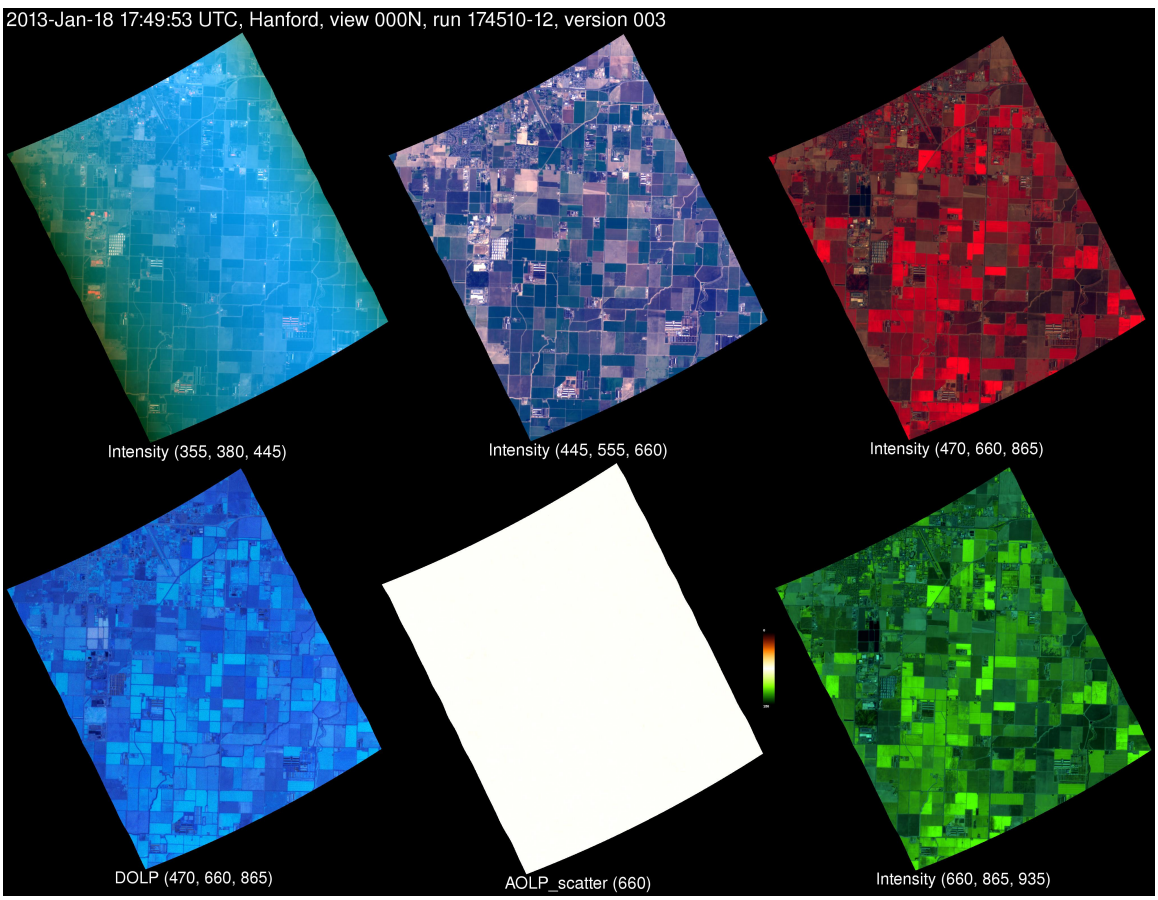

Figure 3. AirMSPI browse product for step-and-stare nadir (00.0°) view over Hanford, CA acquired on 18 January 2013 during the PODEX field campaign.

The images are oriented so that north is to the top of the frame and west is to the left, regardless of the direction of image acquisition. The upper left image shows intensity with B=355, G=380, R=445 nm, highlighting the UV performance of the instrument. This image appears hazy compared to the others due to the enhanced atmospheric scattering in the UV. Note that the absolute calibration in the UV is preliminary as of this release (V001) of the data, which is the reason for the color artifacts at the far right and left edges of the swath. Please consult the Quality Statement for more information. The

Distributed by the Atmospheric Science Data Center
http://eosweb.larc.nasa.gov

upper center image shows intensity with B=445, G=555, R=660 nm, which is a "true color" representation of the scene, similar to what would be seen with the human eye. In this image, it is easy to make out fields, roads, and urban areas. The upper right image shows intensity with B=470, G=660, R=865 nm. This set of wavelengths corresponds to the polarized bands in AirMSPI. Due to the inclusion of the NIR in the red channel, vegetated surfaces appear bright red because of the enhanced reflectance of chlorophyll in this portion of the spectrum. The lower left image is the DOLP in these same three spectral bands. Because DOLP is the ratio of the polarized reflectance to the reflected intensity, care must be taken in interpreting the DOLP images due to the presence of the intensity in the denominator of the ratio. Vegetated fields appear bluish in this image because the enhanced reflectance at the 865 nm wavelength results in smaller DOLP values in the red channel of the image. Water surfaces tend to appear bright in DOLP because of low reflected intensity in all three spectral bands. The image in the bottom center is the angle of linear polarization (AOLP), which is given by the relation, $0.5\tan^{-1}(u/q)$, with u and q both defined relative to the scattering plane. The colorbar ranges from 0° (dark red) through 90° (white) to 180° (dark green). In this scene, the AOLP is consistently white, indicating an angle around 90°, which implies that the value of u is essentially zero and the value of q is negative and non-zero. This means that the light scattered from this scene tends to be polarized perpendicular to the scattering plane. The lower right image shows intensity with B=660, G=865, R=935 nm. The enhanced NIR reflectance in both the 865 nm and 935 nm bands results in the vegetation appearing yellow (G+R=Y).

Individual browse images are available for each stare within the step-and-stare sequence. The histogram scaling is applied to each image independently, however, so comparisons between different views should only be made in a relative sense. In addition, the browse images are cropped to contain just the portion of the scene containing valid AirMSPI data, so sequences of browse images will not necessarily align properly.

3.2.3 KML Product

Besides the browse imagery, Keyhole Markup Language (KML) files are also provided for AirMSPI scenes. KML is the file format used to describe geographic information in Google Earth. Unlike the browse imagery, a single KML file is generated for each target. An example of this is shown in Fig. 4 for the same Hanford target for which the browse image is provided in Fig. 3. Google Earth allows users to interactively visualize the scene by zooming, rotating, and tilting the image. As seen in the figure, the track of the ER-2 aircraft is displayed as a red line. The transparent, green quadrilaterals show each of the nine images acquired for the Hanford target, with the largest ones corresponding to the most oblique view angles and the smallest one corresponding to the nadir view. By opening the folder with the AirMSPI KML filename on the left hand side of the Google Earth browser window labeled "Places," users can toggle on and off different views by checking the appropriate boxes.

Distributed by the Atmospheric Science Data Center
http://eosweb.larc.nasa.gov

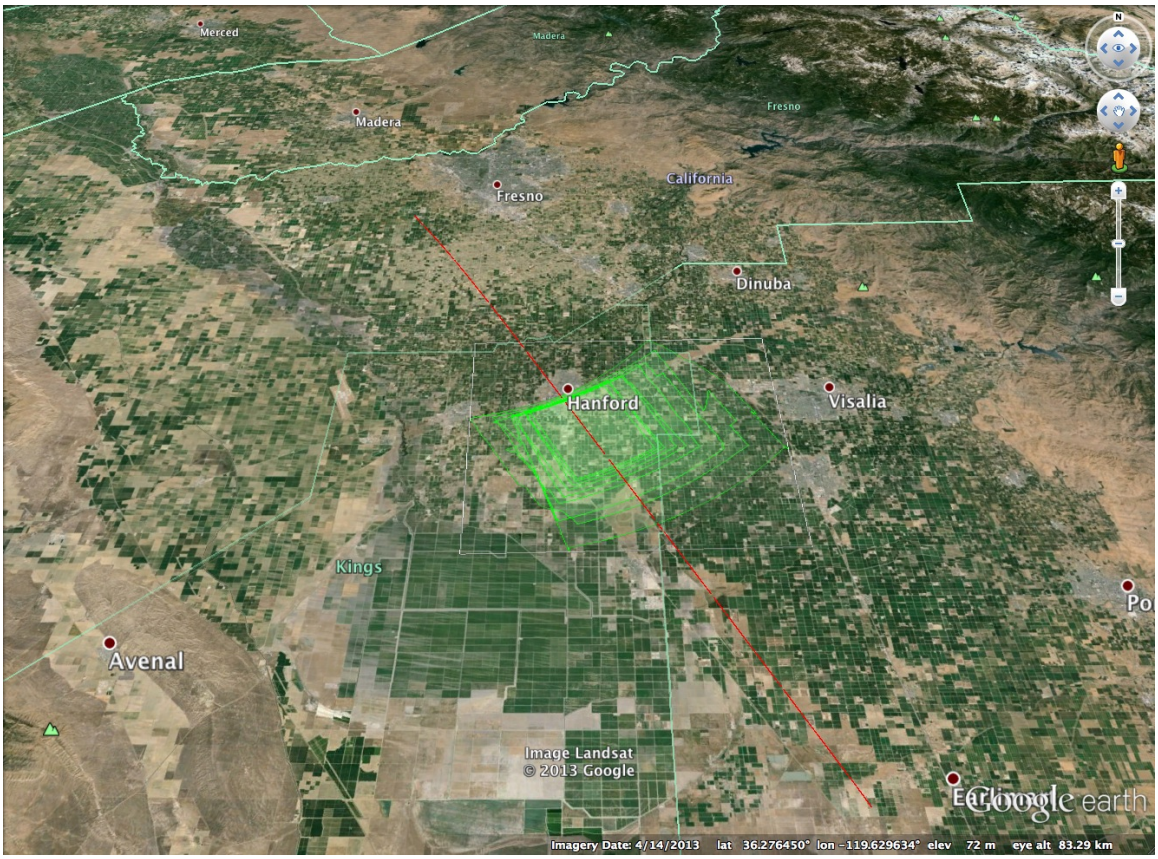

Figure 4. AirMSPI KML product for Hanford, CA acquired on 18 January 2013 during the PODEX field campaign visualized in Google Earth. The red line shows the flight track of the ER-2 aircraft and the green quadrilaterals show the nine individual acquisitions of the Hanford Target.

3.2.4 Single View Angle

This subsection describes the data content of a single AirMSPI L1B2 HDF-EOS-5 format file in manner intended to help users working with the product. For complete details regarding the content of the file, users should consult the Data Product Specification (DPS) for the AirMSPI Level 1B2 Products (JPL D-78958).

3.2.5 Content

The HDF-EOS-5 contents of an AirMSPI file can be viewed using an HDF reader such as HDFView (available from http://www.hdfgroup.org/hdf-java-html/hdfview/). This software provides a graphical user interface for displaying the contents of an AirMSPI file including the hierarchical data structure and file attributes. Additional information on using this software is provided with the application. Note that HDFView does not appear to provide functionality to create images of the AirMSPI data content, so interested users will be required to develop or modify their own software. The examples below were all created using software developed in Interactive Data Language (IDL).

The primary data content is stored in the hierarchy /HDFEOS/GRIDS/ with each spectral band represented by an independent subgroup (e.g., 355nm_band). Figure 5 shows an image created by

Distributed by the Atmospheric Science Data Center
http://eosweb.larc.nasa.gov

reading the hierarchy /HDFEOS/GRIDS/550nm_band/Data Fields/I from the file AirMSPI_ER2_Hanford_GRP_TERRAIN_20130118_174953Z_000N_F01_V003.hdf, which contains the radiant intensity (radiance) for the 555 nm AirMSPI spectral band for the Hanford, CA target acquired during the PODEX field campaign on 18 January 2013 at 17:49:53 UTC from the nadir (00.0°) step-and-stare view. In this case, the radiance (*I*) field has dimensions of 4096 x 3584, represented by the large black area in the figure. Valid (i.e., non-fill) data only occupy a relatively small portion of the total region because the 4096 x 3584 area is designed to be large enough to enclose the image data from all nine stares in the step-and-stare sequence for this particular target. As discussed below, this is done to facilitate multiangle comparisons.

The radiance data are stored as 32-bit floating-point values with a fill value of -999.0, displayed in Fig. 5 as black. The units of radiance are $Wm^{-2}sr^{-1}nm^{-1}$, which is stored as an attribute in the file, and listed in the DPS. In this case, valid values for the radiance units range from 0.0343 to 0.1974. To display an image, these values typically need to be scaled to a standard 8-bit range from 0 to 255. This can be done linearly (e.g., by multiplying by 1291.8, since 0.1974 x 1291.8 = 255) or by using a byte scaling routine. In Figure 4 an automatic histogram stretching algorithm was applied that is similar, but not identical to the algorithm used to generate the browse images discussed in §3.2.2. The color bar was also added using a specially written IDL routine.

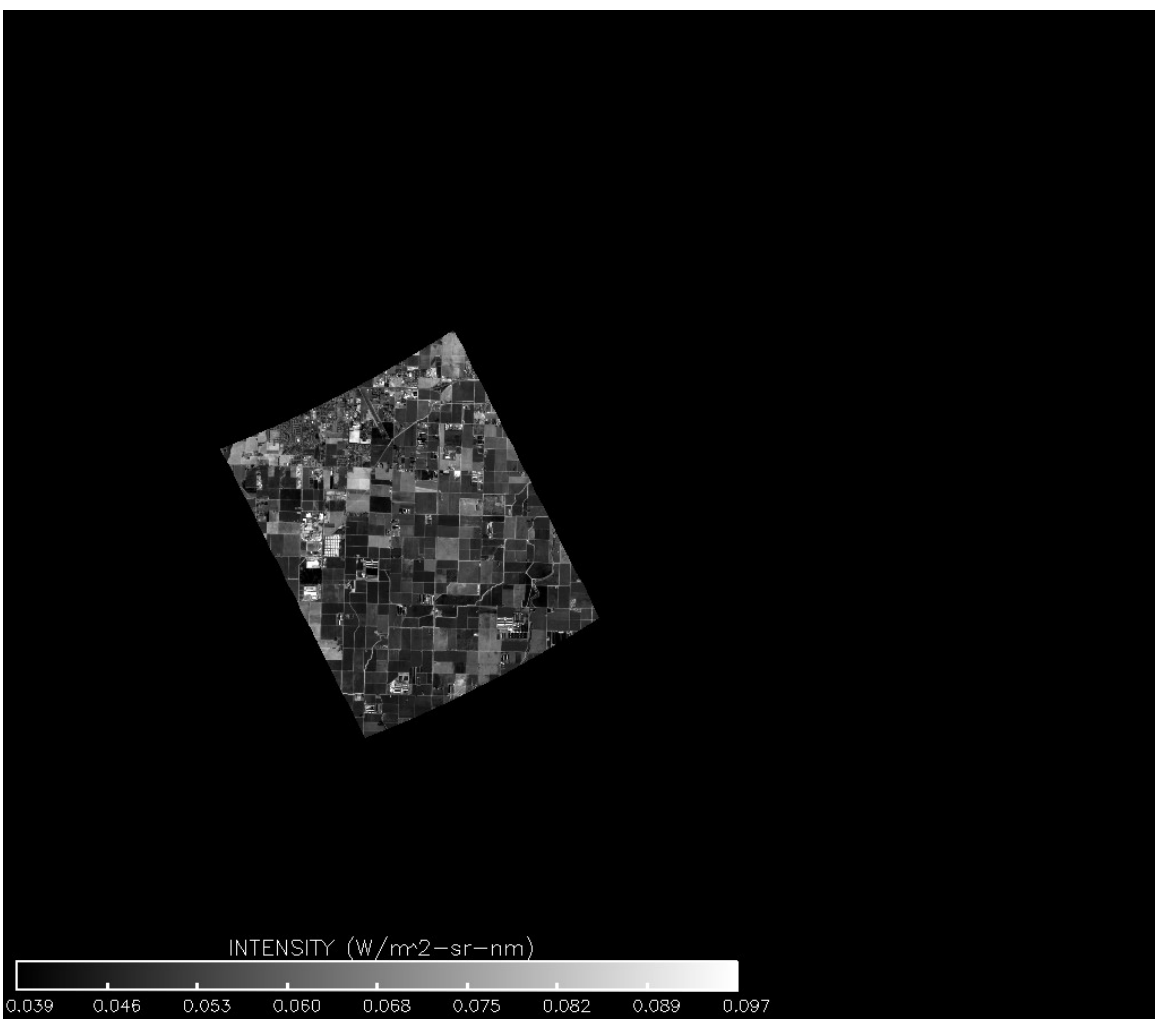

Distributed by the Atmospheric Science Data Center
http://eosweb.larc.nasa.gov

Figure 5. AirMSPI step-and-stare nadir (00.0°) view over Hanford, CA showing radiance in the 555 nm spectral band.

Displaying the data in this manner makes it difficult to see the details of the image due to the presence of the large area of surrounding fill values. Figure 6 shows the same scene, but now displaying only locations containing valid data. The same scaling has been applied in this figure, but locations containing extraneous data have been excluded by testing the x- and y-dimensions for the minimum and maximum values containing valid data. Note that care must be taken to ensure that the correct aspect ratio is maintained in the image (i.e., to ensure that pixels remain square).

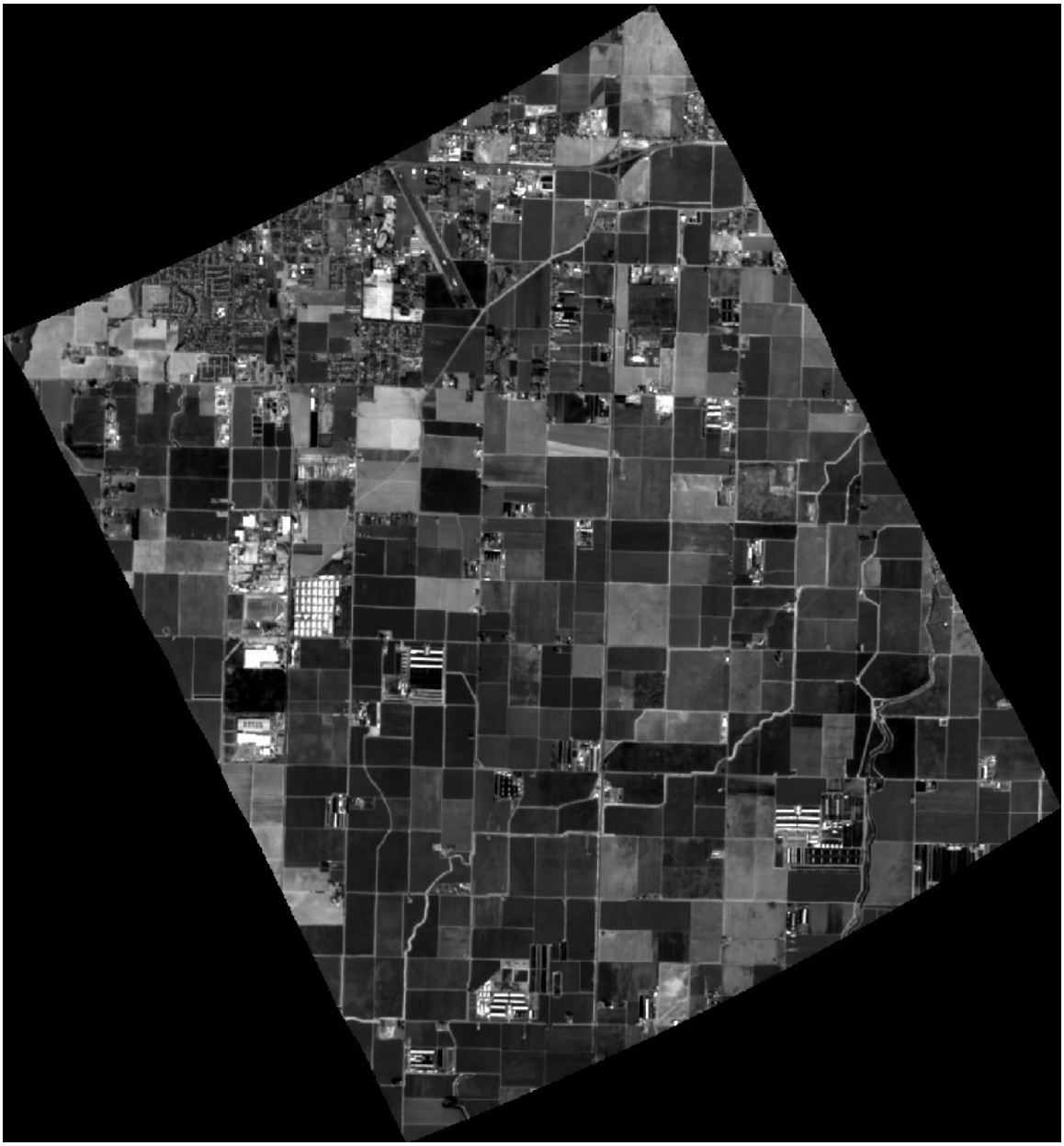

Figure 6. Same as Figure 5, but surrounding fill values have not been included in the image.

Distributed by the Atmospheric Science Data Center
http://eosweb.larc.nasa.gov

3.2.6 Radiometric Data Quality Indicator (RDQI)

The images shown in the previous section were created using the raw radiance (*I*) data contained in the HDF-EOS-5 AirMSPI files. However, users who wish to employ the AirMSPI data in a quantitative sense are encouraged to take into account the radiometric data quality indicators (RDQI) contained within the product as a separate field. Figure 7 shows the Hanford scene at 355 nm with each of the four RDQI levels being applied progressively as a mask to the image. As specified in the AirMSPI DPS, pixels with RDQI = 3 are considered unusable for any purpose. Pixels with RDQI = 2 are considered not usable for science. For the UV band shown in Fig. 7, this includes a number of pixels along the extreme left and right edge of the image where the brightness of the image clearly falls off relative to pixels near the center of the image. Recall that because AirMSPI is a pushbroom imager, a pixel within the line array that is marked as having an RDQI = 2 will sweep out a line in the along-track direction as the image is acquired. Pixels with RQDI = 1 are considered to have reduced accuracy and should be used with caution in scientific applications. In the image in the bottom right of Figure 6 this includes additional pixels within the image itself that may not appear to be visibly to have reduced quality. The remaining pixels with RDQI = 0 are considered to be within specifications. Updates to the RDQI should be expected in future releases of the product. Please consult the AirMSPI Quality Statement for more information on the RDQI and its derivation.

Distributed by the Atmospheric Science Data Center
http://eosweb.larc.nasa.gov

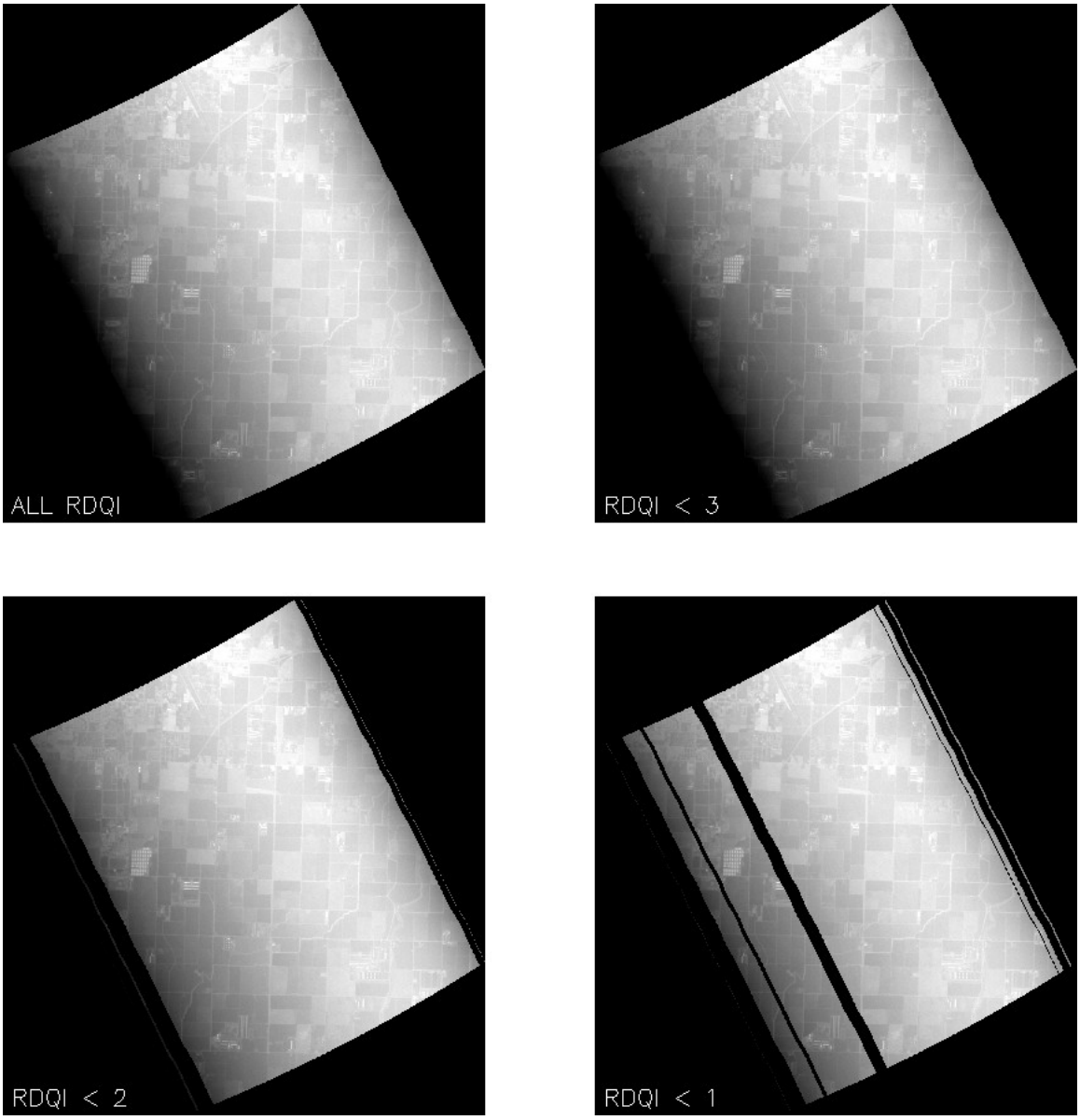

Figure 7. Same scene as Figure 6, but showing the 355 nm (UV) spectral band. Each image applies increasing levels of the RDQI as a mask to screen appropriate pixels. Pixels with RDQI = 0 are considered to be within specifications.

3.2.7 Polarized Intensity and Unit Conversions

In the current (V003) release of the AirMSPI data, the data fields provided include radiance (*I*), degree of linear polarization (DOLP), the polarized intensity (Ipol), the *Q* and *U* components of the Stokes vector in both the meridian (Q_meridian, U_meridian) and the scattering planes (Q_scatter, U_scatter), and the angle of linear polarization in these two planes (AOLP_meridian, AOLP_scatter). Recall that the meridian plane is defined as the plane containing the view vector and the vector normal to the observed surface while the scattering plane is defined as the plane containing the view vector and the solar illumination vector. The radiance (*I*) and polarized radiance (IPol) as well as *Q* and *U* (in both planes) are provided in units of $Wm^{-2}sr^{-1}nm^{-1}$. Because DOLP = $\sqrt{Q^2+U^2}/I$, it is

Distributed by the Atmospheric Science Data Center
http://eosweb.larc.nasa.gov

dimensionless with a value between 0 and 1.

In V003 of the AirMSPI product, the scattering angle, Θ, the glint (or glitter) angle, and associated geometry information are provided for each pixel in the scene for each band independently in units of degrees. The scattering angle is given by the equation:

$$\cos\Theta = -\mu\mu_0 + \nu\nu_0 \cos\Delta\phi\,, \tag{1}$$

where μ and ν are the cosine and sine of the view zenith angle (View_zenith), respectively; μ_0 and ν_0 are the cosine and sine of the solar zenith angle (Sun_zenith), respectively; and $\Delta\phi$ is the relative azimuth angle, given by the absolute value of the difference between the view azimith and solar azimuth angles (View_azimuth – Sun_azimith). The glint angle is given by the equation:

$$\cos\Theta = \mu\mu_0 + \nu\nu_0 \cos\Delta\phi\,, \tag{2}$$

Because the units of *I*, *Q*, *U*, and Ipol depend on the specific characteristics of the detector, it is often advantageous to "normalize" the values relative to some reference, such as a Lambertian surface with the same illumination conditions (c.f., Martonchik et al., 2000). In this case the Bidirectional Reflectance Factor (BRF) is given by:

$$\mathrm{BRF} = \frac{\pi I \times \mathrm{sun_distance}^2}{\mu_0 E_0}\,, \tag{3}$$

where π is the numerical constant, *I* is the radiance, sun_distance represents the current Earth-Sun distance in astronomical units (AU) where 1 AU is the mean Earth-Sun distance, μ_0 is the cosine of the solar zenith angle, and E_0 is the extraterrestrial solar irradiance for the particular AirMSPI band in question. This equation is provided in the file attributes, along with the value for sun_distance, which varies depending on the day of the year. The values for E_0 for each band are contained within the subgroup /HDFEOS/ADDITIONAL/FILE_ATTRIBUTES/Band Table/Solar irradiance at 1 AU. The solar zenith angle is provided for each band as well within its own data field as sun_zenith. Please consult the AirMSPI DPS for more information. As a convenience to the user, the values for the solar irradiance at 1 AU for V003 of the AirMSPI product are provided in Table 1.

Band Number	Wavelength	Solar irradiance at 1 AU
1	355.0	1.009
2	380.0	1.068
3	445.0	1.868
4	470.0	2.0
5	555.0	1.853
6	660.0	1.553
7	865.0	0.972
8	935.0	0.814

Table 1. AirMSPI V001 values for extraterrestrial solar irradiance by band. Note that these values are likely to be updated in later releases of the product.

In a similar manner, Ipol can be converted to the equivalent representation by the calculation:

Distributed by the Atmospheric Science Data Center
http://eosweb.larc.nasa.gov

$$p\mathrm{BRF} = \frac{\pi \mathrm{Ipol} \times \mathrm{sun_distance}^2}{\mu_0 E_0}. \tag{4}$$

3.2.8 Color Images

How to construct color images by combining data from the individual spectral bands, including examples of BRF, pBRF, DOLP, and AOLP.

3.2.9 Navigation

Each pixel in the AirMSPI L1B2 file is associated with a geographic latitude and longitude. This information is contained in the subgroup HDFEOS/GRIDS/Ancillary/Data Fields/Latitude HDFEOS/GRIDS/Ancillary/Data Fields/Longitude. The latitude/longitude grid is common to all single view angles contained within the step-and-stare sequence associated with a specific target.

3.2.10 Multiple View Angles

This subsection describes working with multiple views from the step-and-stare sequence associated with an individual AirMSPI target.

3.2.11 Matching and Overlap

Because the AirMSPI camera has a fixed focal length, the dimensions of the scene increase as the viewing angle increases. L1B2 processing georectifies and projects the data onto a common grid, allowing images from different cameras to be referenced to one another.

3.2.12 Multiangle Spectropolarimetry

By making observations of a single ground location from multiple directions, AirMSPI allows the derivation of the angular nature of light reflected by the atmosphere and underlying surfaces. This information can be used as input into retrieval algorithms that take advantage of the unique content of such observations.

3.3 SWEEP PRODUCTS

This section describes the AirMSPI L1B2 data for the sweep mode.

Distributed by the Atmospheric Science Data Center
http://eosweb.larc.nasa.gov

Distributed by the Atmospheric Science Data Center
http://eosweb.larc.nasa.gov

4 Appendix

4.1 REFERENCES

ACE Science Working Group (2010). Aerosol, Cloud and Ecosystems (ACE) Proposed Satellite Mission Study Report. Available at http://dsm.gsfc.nasa.gov/ace/library.html.

Diner, D.J., L.M. Barge, C.J. Bruegge, T.G. Chrien, J.E. Conel, M.L. Eastwood, J.D. Garcia, M.A. Hernandez, C.G. Kurzweil, W.C. Ledeboer, N.D Pignatano, C.M. Sarture, and B.G. Smith (1998b). The Airborne Multi-angle Imaging SpectroRadiometer (AirMISR): instrument description and first results. *IEEE Transactions on Geoscience and Remote Sensing,* **36**, 1339-1349.

Diner, D.J., A. Davis, B. Hancock, G. Gutt, R.A. Chipman, and B. Cairns (2007). Dual photoelastic modulator-based polarimetric imaging concept for aerosol remote sensing. *Applied Opticts,* **46**, 8428-8445.

Diner, D.J., A. Davis, B. Hancock, S. Geier, B. Rheingans, V. Jovanovic, M. Bull, D.M. Rider, R.A. Chipman, A. Mahler, and S.C. McClain (2010). First results from a dual photoelastic modulator-based polarimetric camera. *Applied Optics,* **49**, 2929-2946.

Diner, D.J., F. Xu, J.V. Martonchik, B.E. Rheingans, S. Geier, V.M Jovanovic, A. Davis, R.A. Chipman, and S.C. McClain (2012). Exploration of a polarized surface bidirectional reflectance model using the Ground-based Multiangle SpectroPolarimetric Imager. *Atmosphere,* **3**, 591-619.

Diner, D.J., F. Xu, M.J. Garay, J.V. Martonchik, B. Rheingans, S. Geier, A. Davis, B.R. Hancock, V. Jovanovic, M. Bull, K. Capraro, R.A. Chipman, and S.C. McClain (2013). The Airborne Multiangle SpectroPolarimetric Imager (AirMSPI): A new tool for aerosol and cloud remote sensing. *Atmospheric Measurement Techniques,* submitted.

Jovanovic, V., B. Ledeboer, M. Smyth, and J. Zong (2001). Georectification of the Airborne Multi-angle Imaging SpectroRadiometer. ISPRS Workshop on High Resolution Mapping from Space, Hannover, Germany.

Jovanovic, V.M., M.A. Bull, M.M. Smyth, and J. Zong (2002). MISR in-flight camera geometric model calibration and georectification performance. *IEEE Transactions on Geoscience and Remote Sensing,* **40**, 1512-1519.

Jovanovic, V. M., M. Bull, D.J. Diner, S. Geier, and B. Rheingans (2012). Automated data production for a novel Airborne Multiangle SpectroPolarimetric Imager (AirMSPI). *International Archives of the Photogrammetry, Remote Sensing and Spatial Information Sciences,* **XXXIX-B1**, 33-38, doi:10.5194/isprsarchives-XXXIX-B1-33-2012.

Distributed by the Atmospheric Science Data Center
http://eosweb.larc.nasa.gov

Kalashnikova, O., M.J. Garay, A.B. Davis, V. Natraj, D.J. Diner, S. Tanelli, and J.V. Martonchik (2011). Sensitivity of multiangle photo-polarimetry to absorbing aerosol vertical layering and properties: Quantifying measurement uncertainties for ACE requirements. Abstract A43F-07 presented at 2011 Fall Meeting, AGU, San Francisco, Calif., 5-9 Dec.

Kawata, Y. (1978). Circular polarization of sunlight reflected by planetary atmospheres. *Icarus*, **33**, 217-232.

Mahler, A., N.A. Raouf, P.K. Smith, S.C. McClain, and R.A. Chipman (2008). Minimizing instrumental polarization in the Multiangle SpectroPolarimetric Imager (MSPI) using diattenuation balancing between the three mirror coatings. Proceedings of SPIE 7013, 701355, doi:10.1117/12.791941.

Mahler, A., D.J. Diner, and R.A. Chipman (2011a). Analysis of static and time-varying polarization errors in the multiangle spectropolarimetric imager. *Applied Optics,* **50**, 2080-2087.

Mahler, A., S. McClain, and R. Chipman (2011b). Achromatic athermalized retarder fabrication. *Applied Optics,* **50**, 755-765.

Martonchik, J.V., C.J. Bruegge, and A.H. Strahler (2000). A review of reflectance nomenclature used in remote sensing. *Remote Sensing Reviews*, **19**, 1-4, 9-20.

Plass, G.N., G.W. Kattawar, and S.J. Hitzfelder (1976). Multiple scattered radiation emerging from Rayleigh and continental haze layers. 2: Ellipticity and direction of polarization. *Applied Optics,* **15**, 1003-1011.

Torres, O., J.R. Herman, P.K. Bhartia, and A. Sinyuk (2002). Aerosol properties from EP-TOMS near UV observations. *Advances in Space Research,* **29**, 1771-1780.

Distributed by the Atmospheric Science Data Center
http://eosweb.larc.nasa.gov

Acronym List

AirMSPI.....Airborne Multiangle SpectroPolarimetric Imager
AOLP ..... Angle of Linear Polarization
ASDC.....Atmospheric Science Data Center
ASL ..... Above Sea Level
AU..... Astronomical Unit
DOLP ..... Degree of Linear Polarization
ECS ..... EOSDIS Core System (Data Production System at DAAC)
EOS ..... Earth Observing System
EOSDIS ..... Earth Observing System Data and Information System
ESDT..... Earth Science Data Type
GCTP ..... General Cartographic Transformation Package
HDF-EOS ..... Hierarchical Data Format for EOS
JPL ..... Jet Propulsion Laboratory
LaRC..... Langley Research Center (NASA)
MISR..... Multi-angle Imaging SpectroRadiometer
NASA..... National Aeronautics and Space Administration
NIR..... Near Infrared
SCF ..... Science Computing Facility
SDP ..... Science Data Processing
UTC ..... Coordinated Universal Time
UTM ..... Universal Transverse Mercator
UV ..... Ultraviolet
VIS ..... Visible

Distributed by the Atmospheric Science Data Center
http://eosweb.larc.nasa.gov